https://erjm.journals.ekb.eg
ISSN: 1110-1180

DOI: ---------

ERJ
Engineering Research Journal
Faculty of Engineering
Menoufia University

Investigation Into Power Generation From a Subway Tunnel Using Wind Turbines

Ahmed S. Saad, Mosaad M. Habib, Mostafa M. Nasr, Abdelfattah Mahrous*

Mechanical Power Engineering Department, Faculty of Engineering, Menoufia University, Egypt
**(Corresponding author: afmahrous@yahoo.com)*

ABSTRACT
Trains inside subways produce high wind gusts that could be converted into useful electrical power using wind turbines. Savonius vertical axis wind turbines have higher self-starting ability, accept wind from all directions, and can be operated using low wind speeds. Accordingly, the main objective of this study is to numerically investigate the performance of a modified design of Savonius rotor to harness the power from subway tunnels. The effect of thickness of rotor blades within the range of 5 to 40 mm will be also studied. The numerical model is based on Reynolds-Averaged Navier-Stokes equations in two dimensions along with the Standard k-ε turbulence model. The rotor performance will be studied in terms of torque and power coefficients in addition to presenting the flow field around the rotor blades. Numerical results showed that the blade with the lowest thickness of 5 mm reaches the steady state condition earlier than all other cases due to its lowest mass and moment of inertia. However, the results showed that the power generated increases as the thickness of the blades increases, until the thickness reaches 30mm, then the power generated becomes almost constant.

Keywords: *Renewable energy; Power generation; Savonius turbine; Subway tunnel; CFD.*

1. Introduction

In the future, the production of power is anticipated to be primarily driven by renewable energy sources due to their environmental friendliness and the depletion of non-renewable resources. Among renewable energy options, wind power stands out, categorized into two main types: horizontal axis wind turbines (HAWTs) and vertical axis wind turbines (VAWTs). VAWTs, specifically, present an opportunity for leveraging high-velocity wind energy generated by passing trains for electricity generation. Various methods have been explored in the past to capture energy from moving trains, with one proposed method involving the installation of energy-harvesting turbines on the train itself. However, implementing such a system could lead to increased aerodynamic drag on the train, which is undesirable as it would result in the loss of more energy than the power generated by the turbines. In the early 1920s, the Savonius vertical axis wind turbine was first developed by a Finish engineer, Savonius [1]. The functioning mechanism of the Savonius rotor relies on the contrast in drag experienced by its two surfaces of rotor blades during rotation around its shaft. This type of rotor offers several benefits, such as its straightforward design, low cost, ability to operate effectively at low wind speeds, capability to harness wind from any direction, and enhanced self-starting capability [2]. Many researchers have conducted numerous experimental and numerical studies to improve its performance. Research on the influence of aspect ratio on rotor performance, as referenced in [3,4], has indicated that aspect ratios ranging from 1.0 to 2.0 yield the best performance outcomes. Moreover, conventional Savonius rotors featuring overlapping blades demonstrate superior initial performance characteristics when contrasted with those lacking such overlap, as indicated in [5]. The number of blades significantly influences the performance of the Savonius rotor, as noted in [6]. Specifically, the two-bladed rotor demonstrates a superior power coefficient compared to the three-bladed rotor. Nevertheless, the three-bladed rotor exhibits a greater initial static torque. Integrating end plates offers a simple means to enhance the performance of traditional Savonius rotors, as highlighted in [7]. For a rotor aspect ratio of 1.0, it is recommended that the diameter of the end plates be 1.1 times the rotor's rotating diameter (D), as referenced in [8]. Guide vanes were utilized as wind

boosters to enhance turbine performance, even in low wind speeds [9]. To enhance the performance of these rotors, one approach is to adjust their blade profiles. The modified blade with elliptical shape shows higher performance compared to the conventional turbine as shown in [10]. According to [11], a rotor featuring elliptically shaped blades with a thickness of 2 mm, an overlap ratio of approximately 0.15, and a separation distance of 7.5 mm demonstrates the most optimal performance. An experimental test has been done to examine the SR3345 and SR5050 blade profiles and comprehend their impact on Savonius wind turbine performance. The wind turbine prototype is placed in front of an open circuit wind tunnel with a velocity of 6 m/s. When a central shaft is fitted, the blades SR3345 and SR5050 attain the best power coefficients at overlap ratios of 0 and 0.18 [12]. In the study referenced by [13], the geometry of the blade profile is determined through the optimization of the section cut angle (θ) of a parabola, ranging from 27.5° to 45°. It is noted that the blade profile produced at θ = 32.5° exhibits a 20% increase in performance coefficient compared to the conventional semicircular blade profile. The blade profile is crafted utilizing a natural cubic spline curve, incorporating fixed endpoints and variable intermediate points, in addition to other parameters. According to the results, at a tip speed ratio of 0.8, the optimized blade profile surpasses the performance of the conventional rotor, achieving a maximum power coefficient that is 23% higher [14]. In reference [15], the approach involves modifying the inner surface of the blade using a wavy profile. Simulation results confirm that at a tip speed ratio of λ=0.4, the power coefficient (Cp) of the wavy rotor exhibits an enhancement of approximately 14.5%. Additionally, it is observed that the peak Cp reaches 0.18 at λ=0.7, indicating a 12.5% improvement compared to the conventional rotor. The grooved surface serves as an effective method to manipulate the surface roughness of a cylinder, which has proven successful in controlling vortex shedding and wake formation behind the cylinder. The study referenced in [16] aims to enhance the aerodynamic performance of a Savonius wind rotor by incorporating a cylinder deflector with various grooved surfaces, serving as a unique deflector system to counteract the adverse effects within the wake zone downstream of the deflector. Results indicate that employing a deflector with a U-grooved surface at a tip speed ratio (TSR) of 0.9 leads to a significant increase in the average power coefficient, by 24.2% and 15.8% respectively, compared to cases without a deflector and those with smooth cylinder deflectors. There would be an extremely unsteady and turbulent flow between the train and the walls of the tunnel. A turbine could be installed to capture the energy of the flow passing through the train's sides in the area between the train and the tunnel walls. Savonius turbines are well-suited for harnessing unsteady wind energy generated by passing trains. They possess higher static torque and can operate effectively at low tip speed ratios [17,18]. The turbine's design and setup are significantly influenced by train aerodynamics. As trains enter and exit tunnels, pressure waves are generated, propagating back and forth along the tunnel's length and impacting the flow around the head and tail sections of the train [19]. This creates highly unsteady and turbulent airflow between the train and the tunnel walls. Based on the above literature, it is noticed that few research was done on power generation from a subway tunnel. Therefore, the main objective of the present study is to investigate the performance of a modified design of Savonius rotor to harness the power from subway tunnels. The effect of thickness of rotor blades within the range of 5 to 40 mm will be also studied. The rotor performance will be studied in terms of torque and power coefficients in addition to presenting the flow field around the rotor blades.

2. Methodology

2.1. Numerical Methodology

In this paper, the simulations are performed to study the 2-D unsteady, incompressible, and turbulent flow around the Savonius wind rotor. The numerical model is based on Reynolds-Averaged Navier-Stokes equations in conjunction with the Standard k-ε turbulence model. The model equations are numerically simulated using ANSYS Fluent software [20]. The governing equations including the continuity and momentum equations can be written in a tensor form as follows [21]:

$$\frac{\partial \overline{u}_i}{\partial x_i} = 0 \tag{1}$$

$$\frac{\partial \overline{u}_i}{\partial t} + \overline{u}_j \frac{\partial \overline{u}_i}{\partial x_j} = -\frac{1}{\rho}\frac{\partial \overline{P}}{\partial x_i} + \frac{\mu}{\rho}\frac{\partial^2 \overline{u}_i}{\partial x_j^2} - \frac{\partial}{\partial x_j}\left(\overline{u_i' u_j'}\right) \tag{2}$$

The equations for the Standard k-ε turbulence model can be found in refs. [22,23].

The Savonius rotor's coefficients of torque (C_T) and power (C_P) can be calculated from the following equations:

$$C_T = \frac{T}{0.5\,\rho\,A\,U^2\,R} \tag{3}$$

$$C_p = \frac{P}{0.5\,\rho\,A\,U^3} \tag{4}$$

Where A is the rotor area, R is the radius of rotor, P is the rotor power, T is the moment of rotor, and ρ is the density of air.

Correlation coefficient (R^2) [24] can be calculated using equations 5 and 6 as given by Maindonald and Braun:

$$R^2 = 1 - \left(\frac{\sum(\emptyset_R - \emptyset_{Pred})^2}{\sum(\emptyset_R - \bar{\emptyset}_R)^2} \right) \quad (5)$$

$$\bar{\emptyset}_R = \frac{\sum_{i=1}^{n} \emptyset_R}{n} \quad (6)$$

Where n is the number of results.

2.2. Rotor geometry

Figure 1 shows the design parameters of a Savonius wind turbine with two semicircular profile blades. In Figure 1, (D) is rotor diameter, (d) blade chord length, with arc angle (Ø), (t) is thickness, and (De) end plate diameter. The investigation was conducted in such that a performance analysis takes place using different thicknesses. All dimensions of the proposed Savonius rotor are presented in Table 1.

Table 1- Dimensions of the proposed Savonius rotor

Endplate diameter (De)	500 mm
Rotor Diameter (D)	450 mm
Blade thickness (t)	5, 10, 15, 25, 30, 35 and 40 mm
Blade arc angle (Ø)	168º

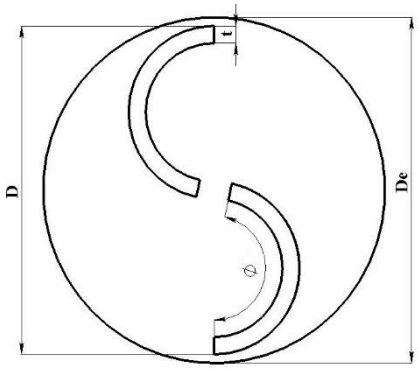

Figure 1- A schematic description of the main geometric parameters of Savonius rotor

2.3. Computational Domain and Boundary Conditions

Computational Domain consists of two main zones: the inner zone, which is rotating, and outer zone, which is stationary, as presented in Figure 2. The outer zone dimensions are 20 D × 5.6 D. The width and length of the train is 3.2 D and 10 D, respectively. The turbine's diameter (D) is 0.5 m. The dimensions of this domain enable the train to make the flow fully developed to the turbine.by assuming that the train is moving when at it was at rest inside the tunnel that is, that trains does not enter or exit tunnels, then the aerodynamics of the train becomes more simpler, the train pushes part of the air in front of it to the sides [25]. Considering a closed-loop construction, the train's motion in the domain is comparable to dynamic similarity in wind tunnel tests. Condition at the boundary of the domain is defined as on the left is the pressure outlet, on the right the velocity inlet. The tunnel (wall 1) and the train (walls 2) are taken as walls with no slip boundary condition, the bottom side is symmetrical plane, and the turbine is rotating walls with no slip boundary condition. The train velocity is considered as 18 m/s. The symmetry criterion is used to reduce the computational time and effort. An interface to link between the rotating and stationary sub-domains is created.

Figure 3 shows how mesh refinement is focused on the wall of the turbine and walls of the train. The entire quantity of mesh elements is about 8×104, consisting of hexahedral cells. Residuals of 1×10-6 have been considered and accomplished in every simulation, indicating that the simulation is well converged. In addition, for simulation, the courant number is less than 0.1 to ensure solution stability. A turbulence intensity of 5% is set up at the inlet.

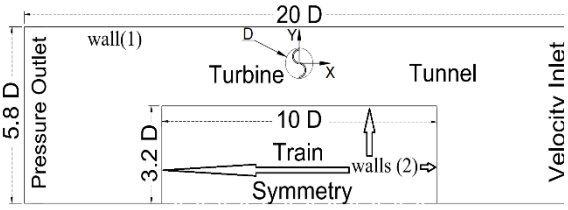

Figure 2- Computational domain and boundary conditions

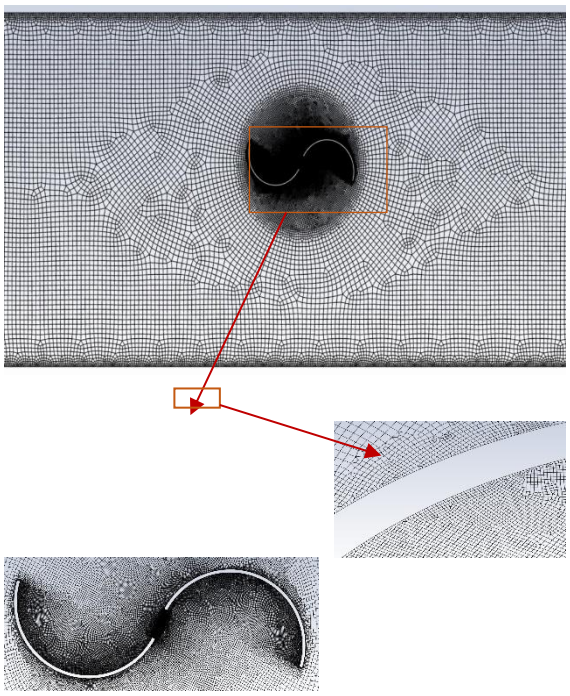

Figure 3- Overview of mesh

2.4. Model Validation

The results of the current CFD simulation are verified by the results of Bethi et al. [26]. Figure 4 displays a comparison of angular velocity as a function of time, as performed in [26] when the rotor diameter = 0.5 m and the distance between the train and turbine = 0.5 m. In Figure4, the numerical results show good agreement compared to the results of ref. [26] with a value of the correlation coefficient (R2) of about 0.99.

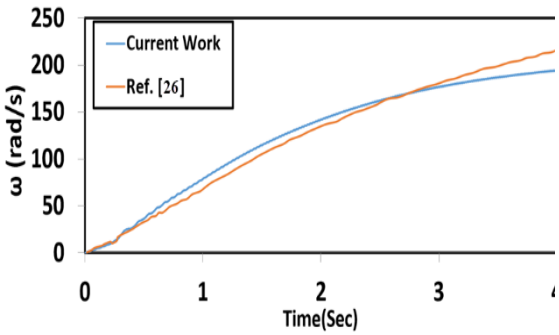

Figure 4- Rotor's angular velocity predicted by current work and result Bethi et al. [26]

3. Results and Discussion

In this section, the effects of various positions of the rotor with respect to length of train in addition to thickness of rotor blades will be presented and discussed.

3.1. Analysis of rotor performance at various local positions

Various rotor positions from the train with respect to longitudinal length (L) in five different locations: at X/L= 0.5, 0.25, 0.0, -0.25, and -0.5, as shown in Figure 5. Figure 6 shows variation of torque coefficient with time (4 seconds) at various rotor position (X/L). The turbine diameter is 0.5 m, and velocity of the train is 18 m/s. The graph shows how position optimization influences rotor performance. The turbine needs to be capable of producing power when positioned next to the train, yet this may not be the best location. When the turbine is put at X/L= 0.5, it achieves a periodic condition with a maximum torque coefficient of 0.78 and a mean coefficient of torque of around 0.22. The rotor does not perform well, yet it can still generate power. At X/L= 0.25 position, a reached periodic condition with a maximum torque coefficient of 0.82 and a mean coefficient of torque of 0.23. The rotor obtained periodic condition with a maximum torque coefficient of around 0.85 and a mean coefficient of torque of 0.24. At X/L= -0.25, the rotor achieves a periodic condition with a maximum torque coefficient of approximately 0.69 and a mean coefficient of torque of 0.23. At X/L= -0.5, the rotor enters a periodic state with a maximum torque coefficient of 0.67 and a mean coefficient of torque of 0.22. In any place except the middle of the rotor. The rotor's low torque during acceleration causes energy loss and lag in achieving a periodic condition. The rotor in the middle of the train performs optimally, with low starting transients and optimal energy harvesting, as shown in Figure 7 and Figure 8, which compares different rotor positions and power generated at each. Figure 7 shows that when the turbine is in the middle position, it has the highest slope of angular velocity vs. time, resulting in the greatest acceleration, as opposed to the low slope achieved in the rear position due to flow behavior across the area between the tunnel and the train.

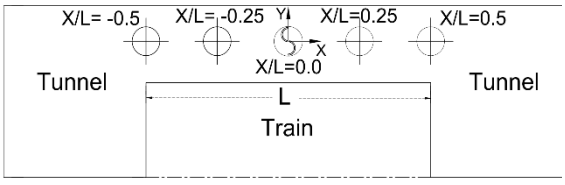

Figure 5- Different positions of turbine

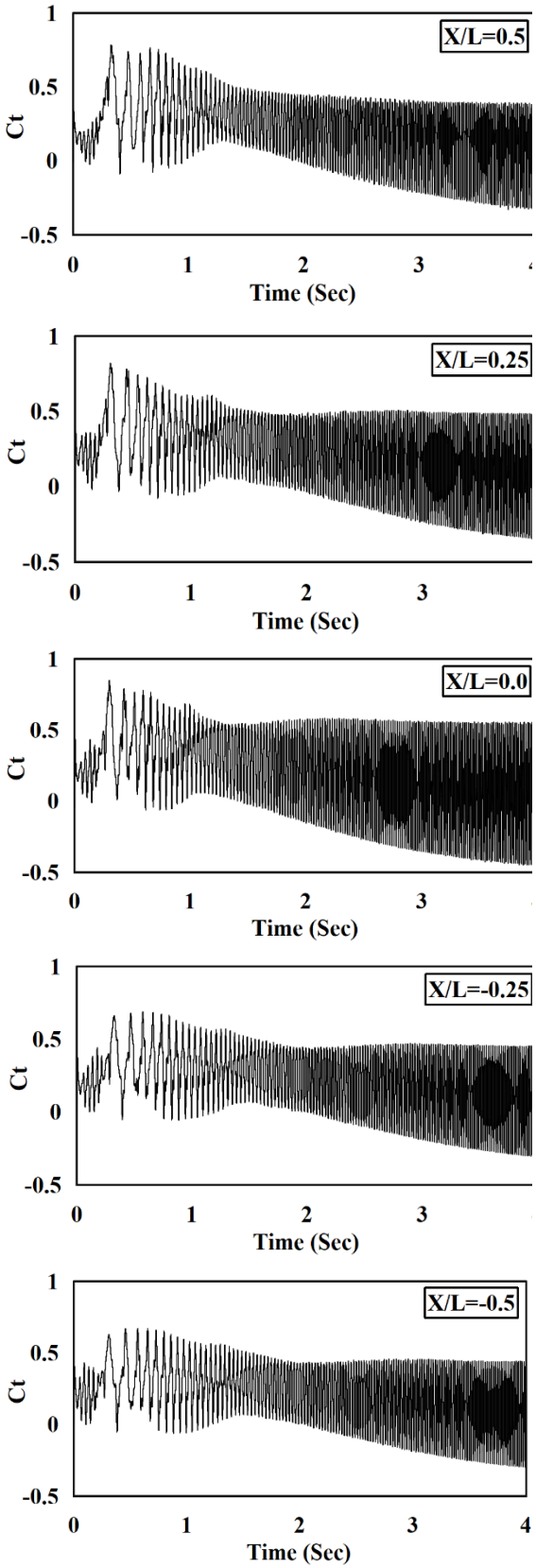

Figure 6- Ct of rotors placed at X/L= 0.5, 0.25, 0.0, -0.25, and -0.5

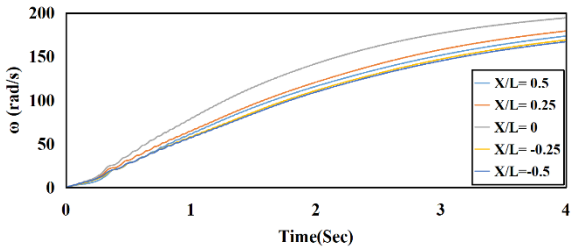

Figure 7- Angular velocity of rotors placed at X/L= 0.5, 0.25, -0.25, and -0.5

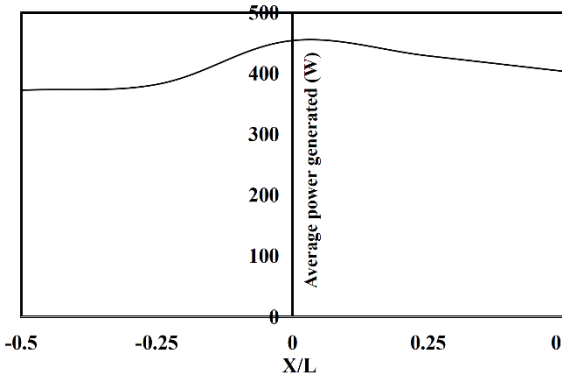

Figure 8- Power generated by rotors placed at X/L= 0.5, 0.25, -0.25, and -0.5

3.2. Thickness of turbine Blades

Figure 9 displays the effect of rotor blade thickness on seven different thicknesses: 5mm, 10mm, 15mm, 25mm, 30mm, 35mm, and 40mm. The turbine with 0.5 m diameter, and the train's velocity is 18 m/s. The graph shows how thickness optimization influences rotor performance. When the thickness of turbine blades is 5mm, it obtains a periodic condition at t = 0.22s with a maximum torque coefficient of 0.68 and a mean torque coefficient of about 0.067. Figures 12 and 13 shows flow visualization of velocity and pressure contours around rotor domain. The rotor does not perform well, yet it can still generate power. At a thickness of 10 mm, it achieves a periodic condition at t = 0.25s, with a maximum torque coefficient of 0.79 and a mean torque coefficient of around 0.12. Maximum torque coefficient of 0.79, with a mean torque coefficient of roughly 0.17 when blade thickness is 15 mm. When the turbine blade thickness is 25mm, the maximum torque coefficient is 0.82, whereas the mean torque coefficient is approximately 0.25. When utilizing a thickness of 30mm, the maximum torque coefficient is 0.82, while the mean torque coefficient is approximately 0.266. Using a thickness of 35 mm, the maximum torque coefficient

is 0.82, whereas the mean torque coefficient is approximately 0.28. With a thickness of 40mm, the maximum torque coefficient is 0.82, whereas the mean torque coefficient is approximately 0.3. Figure 10 shows the fluctuation in angular velocity over time at various thicknesses. Figure 10 indicates that the blade with a thickness of 5 mm reaches the steady state earlier than all other cases due to its lowest mass and lowest moment of inertia among the other cases. Figure 11 shows the power generated at various blade thicknesses. The results show that the power generated increases as the thickness of the blades increases, until the thickness reaches 30mm, then the power generated becomes almost constant. Figure 12 and 13 present velocity and pressure contours, respectively for rotor with thickness of 5 mm at t=1, 2, 3, and 4 seconds.

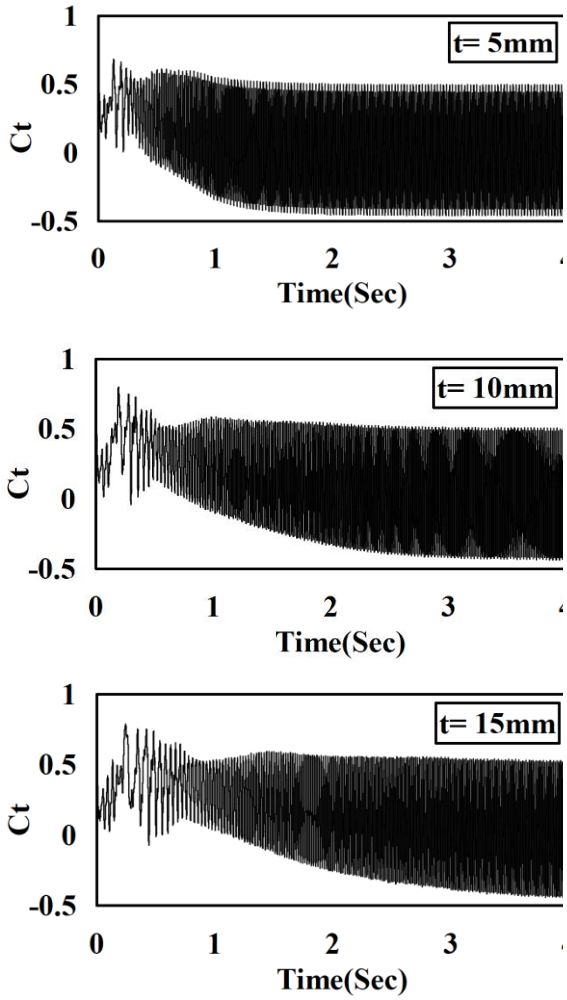

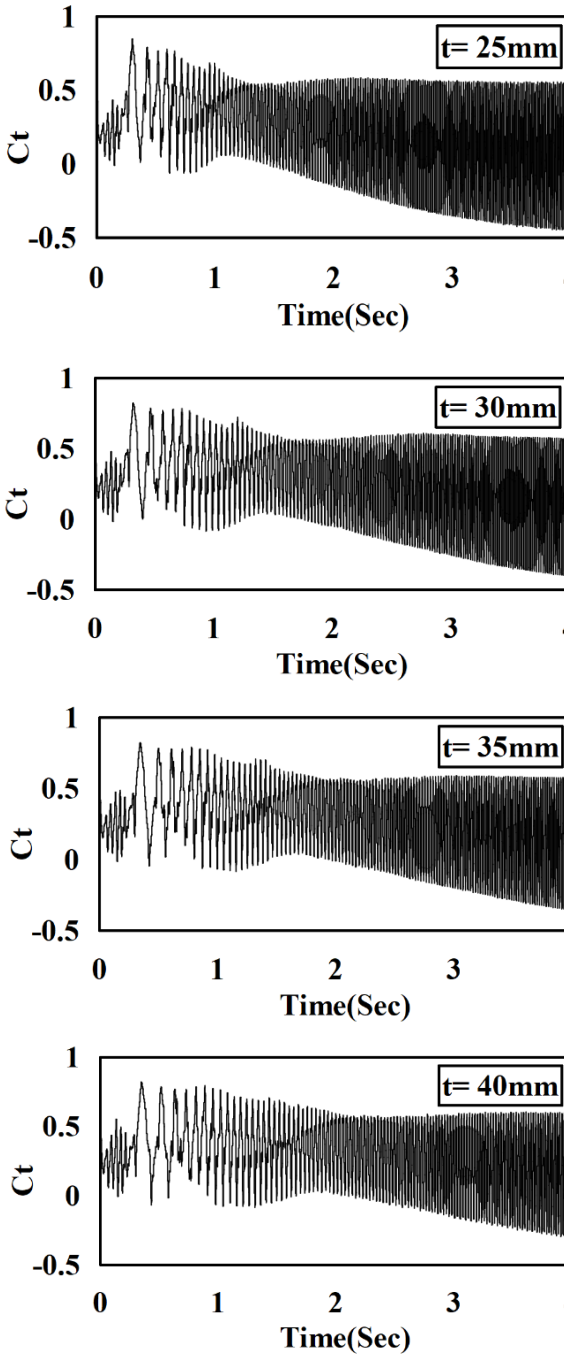

Figure 9- Ct of rotors of different thicknesses of 5, 10, 15, 25, 30, 35, and 40mm

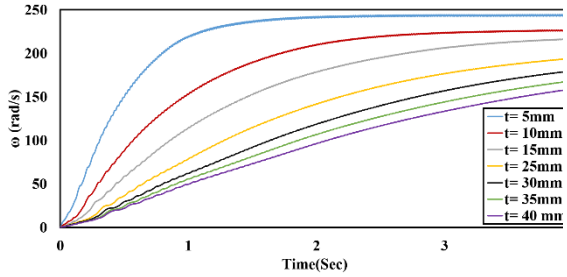

Figure 10- Angular velocity of rotors of different thicknesses of 5, 10, 15, 25, 30, 35, and 40mm.

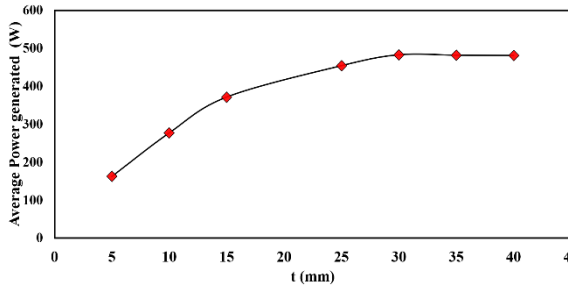

Figure 11- Power generated by rotors with different thickness values.

At t=1 sec

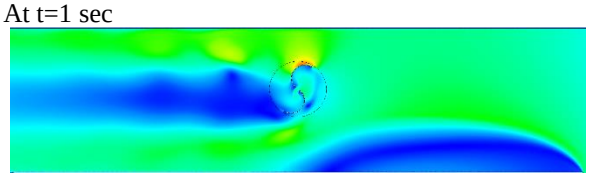

At t=2 sec

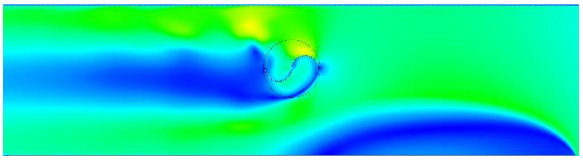

At t=3 sec

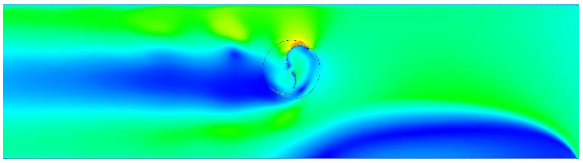

At t=4 sec

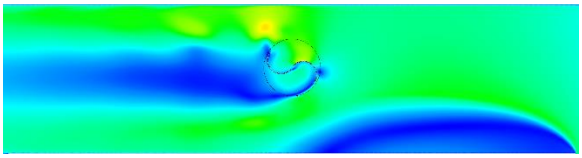

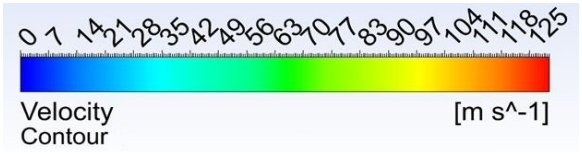

Figure 12- Velocity contours for rotor with thickness of 5mm

At t=1 sec

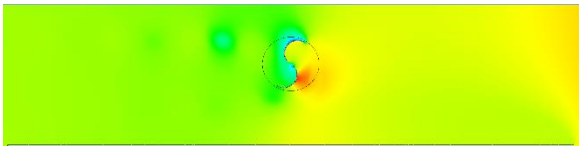

At t=2 sec

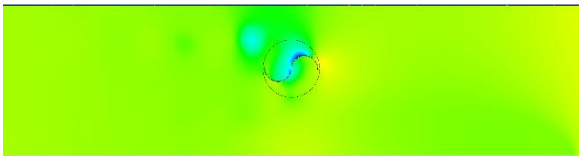

At t=3 sec

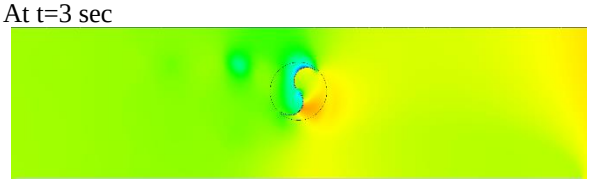

At t=4 sec

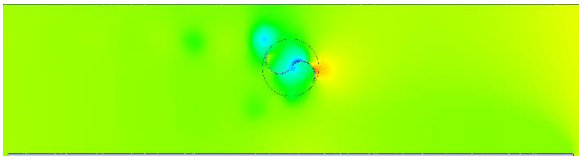

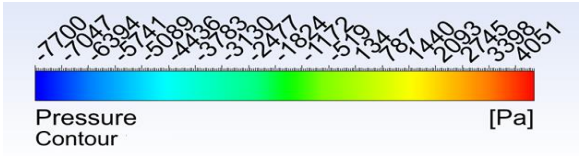

Figure 13- Pressure contours for rotor with thickness of 5mm

4. Conclusions

The performance of a modified design of Savonius rotor to harvest the power from subway tunnels is numerically studied. The influence of various rotor blade thickness within the range of 5 to 40 mm is also investigated. The numerical simulations are carried out based on two-dimensional, turbulent, and unsteady Reynolds-Average Navier-Stokes equations along with the Standard k-ε turbulence model. The results predicted by the current numerical model are successfully validated with data from the literature. The rotor performance in terms of torque and power coefficients in addition the flow field around the rotor blades is calculated and presented.

Predicted results revealed that the blade with the lowest thickness of 5 mm reaches the steady state condition earlier than all other cases due to its lowest mass and moment of inertia. However, the results showed that the power generated increases as the thickness of the blades increases, until the thickness reaches 30mm, then the power generated becomes almost constant. The results presented in this paper could be beneficial in expanding the knowledge of how to produce power from vehicles in motion inside subway tunnels.

References

[1] Ushiyama, I., & Nagai, H. (1988). Optimum design configurations and performance of Savonius rotors. Wind Engineering, 59-75.

[2] Akwa, J. V., Vielmo, H. A., & Petry, A. P. (2012). A review on the performance of Savonius wind turbines. Renewable and sustainable energy reviews, 16(5), 3054-3064.

[3] Bhayo, B. A., & Al-Kayiem, H. H. (2017). Experimental characterization and comparison of performance parameters of S-rotors for standalone wind power system. Energy, 138, 752-763.

[4] Akwa, J. V., da Silva Júnior, G. A., & Petry, A. P. (2012). Discussion on the verification of the overlap ratio influence on performance coefficients of a Savonius wind rotor using computational fluid dynamics. Renewable energy, 38(1), 141-149.

[5] Nasef, M. H., El-Askary, W. A., Abdel-Hamid, A. A., & Gad, H. E. (2013). Evaluation of Savonius rotor performance: Static and dynamic studies. Journal of Wind Engineering and Industrial Aerodynamics, 123, 1-11.

[6] Mohamed, M. H., Janiga, G., Pap, E., & Thévenin, D. (2011). Optimal blade shape of a modified Savonius turbine using an obstacle shielding the returning blade. Energy Conversion and Management, 52(1), 236-242.

[7] Jeon, K. S., Jeong, J. I., Pan, J. K., & Ryu, K. W. (2015). Effects of end plates with various shapes and sizes on helical Savonius wind turbines. Renewable energy, 79, 167-176.

[8] Kamoji, M. A., Kedare, S. B., & Prabhu, S. V. (2009). Performance tests on helical Savonius rotors. Renewable Energy, 34(3), 521-529.

[9] El-Askary, W. A., Nasef, M. H., Abdel-Hamid, A. A., & Gad, H. E. (2015). Harvesting wind energy for improving performance of Savonius rotor. Journal of Wind Engineering and Industrial Aerodynamics, 139, 8-15.

[10] Mrigua, K., Zemamou, M., & Aggour, M. (2022). Numerical Investigation of a New Modified Savonius Wind Turbines. International Journal of Renewable Energy Development, 11(4).

[11] Kaya, A. F., & Acır, A. (2022). Enhancing the aerodynamic performance of a Savonius wind turbine using Taguchi optimization method. Energy Sources, Part A: Recovery, Utilization, and Environmental Effects, 44(2), 5610-5626.

[12] Hosseini, S. E., & Salehi, F. (2023). Analyzing overlap ratio effect on performance of a modified Savonius wind turbine. Physics of Fluids, 35(12).

[13] Mohan, M., & Saha, U. K. (2023). Computational study of a newly developed parabolic blade profile of a Savonius wind rotor. Journal of the Brazilian Society of Mechanical Sciences and Engineering, 45(10), 548.

[14] Mohan, M., & Saha, U. K. (2024). Evolving a Novel Blade Shape of a Savonius Wind Rotor Using an Optimization Technique Coupled with Numerical Simulations and Wind Tunnel Tests. Journal of Energy Resources Technology, 146(4).

[15] Al-Ghriybah, M., & Didane, D. H. (2023). Performance improvement of a Savonius wind turbine using wavy concave blades. CFD Letters, 15(9), 32-44.

[16] Fatahian, E., Ismail, F., Ishak, M. H. H., & Chang, W. S. (2023). Aerodynamic performance improvement of Savonius wind turbine through a passive flow control method using grooved surfaces on a deflector. Ocean Engineering, 284, 115282.

[17] Zhou, T., & Rempfer, D. (2013). Numerical study of detailed flow field and performance of Savonius wind turbines. Renewable energy, 51, 373-381.

[18] Alexander, A. J., & Holownia, B. P. (1978). Wind tunnel tests on a Savonius rotor. Journal of Wind Engineering and Industrial Aerodynamics, 3(4), 343-351.

[19] Raghu S Raghunathan, H.-D.K., T Setoguchi, Aerodynamics of high-speed railway train, Progress in Aerospace Sciences, 2002. 38(6-7): p. 469-514.
[20] Fluent. User's Guide Fluent 19.0. Fluent Incorporated, Lebanon, NH.2019
[21] Saad, A.S., El-Sharkawy, I.I., Ookawara, S. and Ahmed, M., 2020. Performance enhancement of twisted-bladed Savonius vertical axis wind turbines. Energy Conversion and Management, 209, p.112673.
[22] Dhamotharan, V., Jadhav, P. D., Ramu, P., & Prakash, A. K. (2018). Optimal design of savonius wind turbines using ensemble of surrogates and CFD analysis. Structural and Multidisciplinary Optimization, 58, 2711-2726.
[23] Setiawan, P. A., Yuwono, T., & Widodo, W. A. (2018, November). Numerical simulation on improvement of a Savonius vertical axis water turbine performance to advancing blade side with a circular cylinder diameter variation. In IOP Conference Series: Earth and Environmental Science (Vol. 200, No. 1, p. 012029). IOP Publishing.
[24] Maindonald, J., & Braun, J. (2006). Data analysis and graphics using R: an example-based approach (Vol. 10). Cambridge University Press.
[25] Khayrullina, A., Blocken, B., Janssen, W., & Straathof, J. (2015). CFD simulation of train aerodynamics: train-induced wind conditions at an underground railroad passenger platform. Journal of Wind Engineering and Industrial Aerodynamics, 139, 100-110.
[26] Bethi, R. V., Laws, P., Kumar, P., & Mitra, S. (2019). Modified Savonius wind turbine for harvesting wind energy from trains moving in tunnels. Renewable energy, 135, 1056-1063.